Instrument Science Report WFC3 2007-027

WFC3 TV2 Testing: UVIS-2 Read Noise

A.R. Martel & S. Baggett
November 27, 2007

ABSTRACT

We examine the read noise of the spare UVIS-2 detector of the Wide Field Camera 3 during its second thermal vacuum campaign at the Goddard Space Flight Center. Only the frames acquired in the default readout mode are considered : a gain = 1.5 e^-/DN, a four amplifier readout (ABCD), and no on-chip binning. The read noise is calculated from the serial virtual overscan region of each quadrant. From a sample of ~600 frames at an operating temperature of -78 C, the read noise is 3.17± 0.02, 3.15± 0.08, 3.20 ± 0.03, and 3.27 ± 0.02 e^- for amplifiers A, B, C, and D, respectively. At a temperature of -81 C (and from a smaller sample), the read noise is lower by ~0.6% for amps A and B and by ~1.4% for amps C and D. A weak positive correlation is found between the read noise and the median level of the imaging areas for amps C and D, possibly from a non-perfect serial transfer of the charge. The variation is very small, roughly 0.05 e^- (1.5%) or less over a range of imaging levels of 10000 e^- to 60000 e^-. Similarly, a weak negative correlation is found for amplifiers A and B. The CEI specification of a read noise of < 4 e^- is easily met for an operating detector temperature of < -20 C. There is no difference in the read noise between instrument sides 1 and 2. In an appendix, we present and analyze the superbias frame. A weak residual odd/even effect is observed in each quadrant and the ovsercan regions. The peak-to-peak amplitude of the effect is 0.01-0.03 e^- for amps A,C,D and ~0.4 e^- for amp B. The presence of this pattern will be checked for the flight detector and if necessary, proper modifications to calwf3 will be explored to minimize its impact.

Introduction

The Wide Field Camera 3 (WFC3) underwent its second thermal vacuum campaign, TV2, during the summer and fall of 2007. During this period, the instrument was placed in the Space Environment Simulation (SES) Chamber at the Goddard Space Flight Center (GSFC). The Calibrated Stimulus from Leftover Equipment (CASTLE) delivered external light stimuli into WFC3, in particular monochromatic and broad-band point source and flat field illumination, by using a combination of fibers, lamps, and laser diodes while closely simulating the optical path and aberrations of the Hubble Space Telescope (HST).

During TV2, approximately sixteen thousand frames were acquired for both the UVIS and IR channels. For this report, we have assembled a sub-sample of several hundred frames to calculate the read noise of the four amplifiers of the spare UVIS-2 detector (CCD40 - amplifiers C and D, CCD50 - amplifiers A and B), which was installed in the instrument for the entire duration of the TV2 campaign. We treat only the frames with the default on-orbit readout mode : four amplifiers (ABCD), a gain of 1.5 e^-/DN, and no on-chip binning. Prior efforts to characterize the read noise of the UVIS-2 detector have been documented in Baggett (2007a) but for the ambient environment of the Space Systems and Integration Development Facility (SSDIF) at GSFC and at a detector temperature of -54 C. In the following, we present our sample choice, our method of analysis, and our results.

Data

For this study of the read noise of the CCDs of the WFC3 UVIS-2 detector, we consider the frames acquired in the default on-orbit configuration : a four amplifier readout (ABCD), a gain of 1.5 e^-/DN, and no on-chip binning (1x1). The frames span the entire duration of the Thermal Vacuum 2 (TV2) campaign, which was bracketted by an abbreviated and full Servicing Mission Functional Test in ambient conditions after the instrument was moved into the SES and before it was removed. This entire period covers Jun 11, 2007 (day of year 162) to Oct 14, 2007 (day of year 287) and the corresponding ID numbers of the frames in the WFC3 ground database are 29067 to 44865.

Several images had to be rejected. Some were taken in special modes, such as EPER, that produced non-standard image dimensions and overscan regions. Others were simply missing from the database while several possess corrupted FITS headers, sometimes resulting from a glitch in the data dump or from a mismatched CASTLE stimulus file. These amounted to a total of 38 frames.

In several cases, the readnoise from amplifier B was found to be inordinately large (several thousands of counts). An examination of the images indicates that these high values are due to saturation in quadrant B, which spilled into the virtual overscan. The problems in the gate voltages of amplifier B and the resultant fix have been documented in Baggett & Waczynski (2007). Martel (2007) also notes that the characteristics of the dark current of this amplifier is the most problematic of the four : it exhibits the highest dark current rate and the heaviest hot pixel population and hot pixel rate. A total of 34 frames were affected by the amp B anomaly and were thus excluded from this study. But the frames that served to characterize and resolve this issue, using revised gate voltages, were included since their gain and read noise appear to differ little from the non-corrected values (Baggett & Waczynski 2007).

Our final tally of frames in this report consists of 618 frames. Of these, 164 (27%) and 70 (11%) are bias and dark frames, respectively. The images were acquired over a range of detector temperatures, as defined by the IUVDETMP keyword, throughout the TV2 campaign; this permits a characterization of the temperature dependence of the noise. A lien against the detector did not allow operation at the on-orbit temperature of -83 C. Hence, the vast majority of the sample, 480 frames (78 %), was acquired at ~-78 C (more precisely, from -77.72 C to -78.65 C). Ten (1.6 %) frames were acquired at ~-81 C. In the following, we will also separate the sample by instrument side or Main Electronics Box (MEB 1 or 2), to determine if one side generates more noise than the other in the UVIS-2 detector.

Analysis

All images are processed with a Python class written by one of us (Martel). One of the methods defined in the class calculates basic statistical quantities (minimum, maximum, mean, median, RMS noise) on all the imaging areas and overscan regions of the two CCDs and writes the results to a file. These are then translated from counts (or digital numbers, DNs) to e^- using the gains tabulated in Baggett (2007b). For gain=1.5, these are 1.57, 1.54, 1.63, and 1.59 e^-/DN for amplifiers A, B, C, and D, respectively. For the purposes of this report, the RMS noise in the serial virtual overscan serves as our measure of the read noise. In previous studies (e.g. Baggett 2007a), the WFC3 UVIS noise has also been characterized using the imaging area pixels.

Results

Temperature Dependence

The temperature dependence of the read noise is shown in Fig. 1. It is well described by a 4th-order polynomial, also shown. The Contract-End-Item specification of a read noise less than 4 e^- is met for temperatures colder than -20 C.

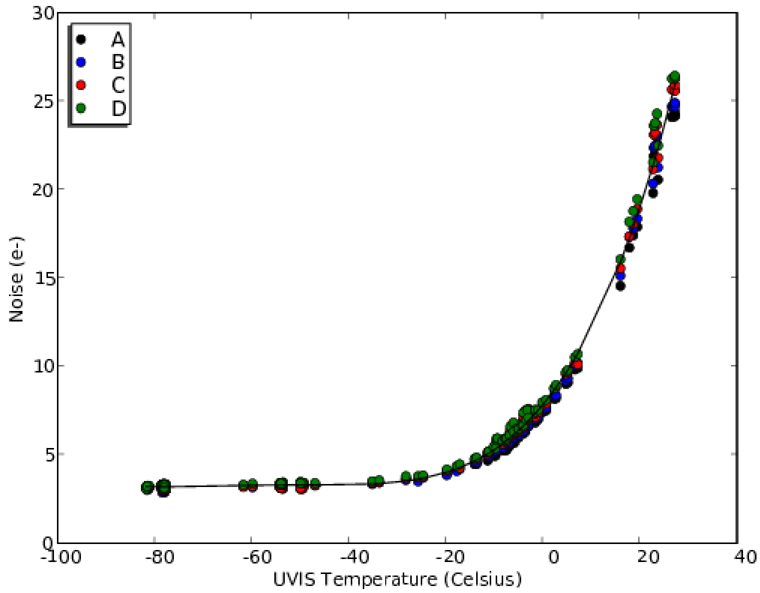

Figure 1 : Temperature dependence of the read noise of all the frames acquired in TV2 in standard configuration (ABCD readout, gain=1.5, and no binning). The solid line is a 4th-order polynomial fit to the combined data points.

Stability at -78 C

In Fig. 2, we plot the read noise of each amplifier as a function of the day the frame was obtained. Only operating temperatures of ~-78 C are considered. This dataset essentially spans the duration of the core of TV2, ~100 days or 3.3 months. Although there are gaps in the time sampling, reflecting the variety of activities over such a long campaign, we find no long term trends in the behavior of the read noise for any of the amplifiers. The noise is well constrained within a band of 3.0 e^- to 3.3 e^-.

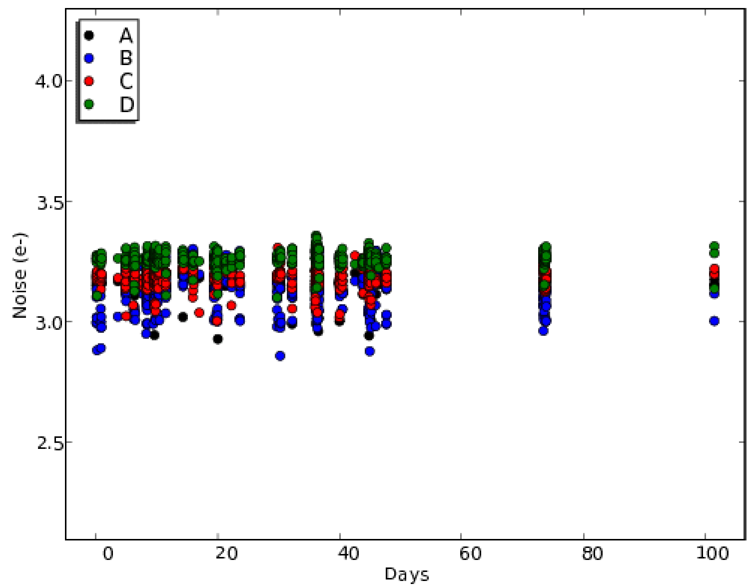

Figure 2 : The read noise of all the frames in our sample at ~-78 C as a function of the day in TV2. The first image at -78 C corresponds to Day 0.

Noise Distributions at -78 C

Histograms of the noise distributions for all the frames at ~-78 C are shown in Fig. 3. These are essentially 'collapsed' versions of Fig. 2 along the horizontal axis. Gaussian fits are also overplotted. We choose the location of the peak of the Gaussian as the read noise and the standard deviation of the distribution as the error on the noise. These quantities are listed in Table 1.

The noise distributions are varied and some possess considerable structure. In particular, amp A shows the narrowest and smoothest distribution. On the other hand, the amp B distribution is the worst of all four amps - it shows several peaks, the most scatter, and is not well represented by a Gaussian. This bad behavior is probably not unexpected given the already mentioned problems with the saturation level, dark current, and hot pixels of this amplifier and its quadrant (see above). Curiously, the amp C distribution, and perhaps also the amp D distribution, appear double peaked.

To gain some insights into the shape of the histograms, we plot the read noise of each amplifier against the median level of its imaging area in Fig. 4. The median level is calculated in a 1000x1000 box centered on each quadrant to avoid any possible edge effects. Although the data are largely concentrated in two clusters, <10000 e^- and >40000 e^-, there appears to be a positive correlation for the CD chip and a negative correlation for the AB chip. The correlations remain even if the size of the virtual overscans is modified. An analysis using Pearson's correlation coefficient indicates that the linear relationships are weak but significant : *r* = -0.50, -0.36, 0.25, and 0.74 for amps A, B, C, D, respectively. We note that even for amp D, the change in the read noise over the full range of the imaging area (10000 e^- to 60000 e^-, say) is very small, < 0.05 e^- or 1.5%. The observed correlations could be due to a non-perfect serial transfer of the accumulated charge, resulting in a ‘leak’ between the imaging area and the serial virtual overscan region (private communicate, A. Waczynski). This ‘spillage’ was also noted by Robberto (2007) when computing the Charge Transfer Efficiency (CTE).

The non-uniform sampling of the absolute levels of the imaging areas likely explains the structure in the noise histograms. For amp C, the peak at ~3.17 e^- appears to correspond to the data points below a level of 10000 e^- while the peak at ~3.20 e^- results from the cluster at > 40000 e^-. A more uniform sampling, filling the gap between 20000 e^- and 40000 e^-, for example, would likely remove the double peak and produce a smoother noise distribution. A similar argument can be made for the peaks at ~3.27 e^- and ~3.30 e^- for amp D. The large scatter of the amp B data over all levels of the science areas explains its erratic and broad noise distribution. By contrast, the amp A data show the smallest scatter, reflected in the narrow noise histogram of this amplifier.

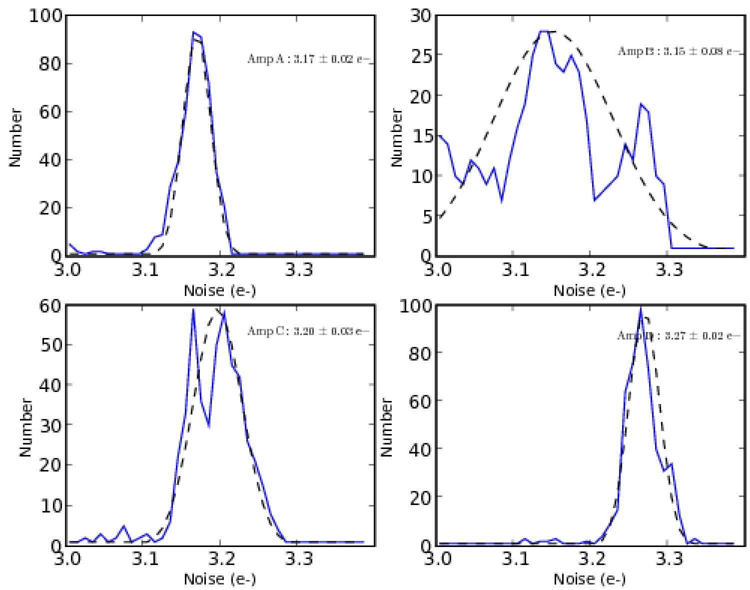

Figure 3 : Histograms of the read noise of all the frames acquired in TV2 in standard configuration (ABCD readout, gain=1.5, and no binning).

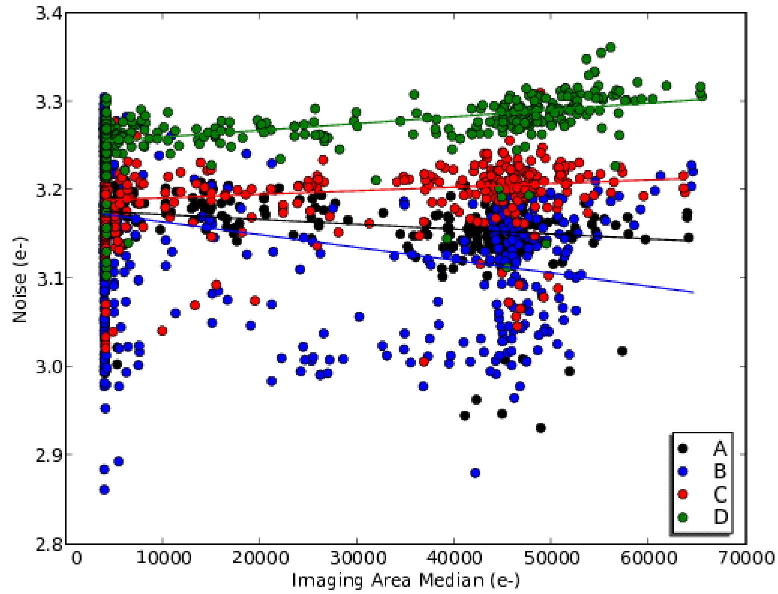

Figure 4 : The read noise is plotted against the median level of the imaging area for each amplifier. Linear fits are shown as solid lines. Data points that deviate by more than 2 sigmas from the mean are excluded from the fits.

Bias Frames

Given the dependence of the read noise on the absolute level of the imaging areas at -78 C, the bias frames should presumably exhibit the lowest read noise. We processed the bias frames in the same manner as the entire dataset. Unfortunately, the resulting uncertainties on the bias read noise are of the same magnitude as the observed linear correlation, a few hundredths of an e^-. Hence, within the uncertainties, the read noise of the bias frames is identical to the read noise of the entire dataset at ~-78 C.

Read Noise at -81 C

Only ten full frames (ABCD readout, gain=1.5 and no binning) are available at an operating temperature of ~-81 C, close to the nominal on-orbit temperature, The mean and standard deviation of the read noise at this temperature are listed in Table 1. The read noise of the AB and CD chips at -81 C are ~0.6% and 1.4% lower than at -78 C, respectively.

Table 1 : Read Noise of the UVIS-2 Detector in Standard Readout Mode

Temperature	**A**	**B**	**C**	**D**
-78 C	3.17 ± 0.02	3.15 ± 0.08	3.20 ± 0.03	3.27 ± 0.02
-81 C	3.15 ± 0.05	3.13 ± 0.06	3.16 ± 0.01	3.22 ± 0.05

Differences between Instrument Sides 1 and 2

The full dataset at -78 C was separated between sides 1 and 2 using the MEBID keyword. We find that the read noise of each amplifier agrees very well between the two sides (within 0.01 e^-) and is essentially identical to the read noise of the full dataset listed in Table 1. Hence, the MEB has no effect on the read noise of the UVIS-2 detector.

Conclusions

We have characterized the read noise of the spare UVIS-2 detector of WFC3 using several hundred frames acquired in TV2. For an operating temperature of -78 C, we have examined the stability of the noise over 100 days, its temperature dependence, its distribution, and its correlation with the absolute level of the imaging area. A few frames at -81 C were also examined. A similar analysis of the noise will be performed for the flight detector in the third thermal vacuum campaign currently scheduled in the winter and spring of 2008.

References

Baggett, S. 2007a, ISR 2007-15: WFC3 Ambient-2 Testing: UVIS Readnoise

Baggett, S. 2007b, ISR 2007-19: WFC3 TV2 Testing: UVIS-2 Gain Results

Baggett, S. & Waczynski, A. 2007, ISR 2007-22: WFC3 TV2 Testing: UVIS-2 Amp B Anomaly

Martel, A.R. 2007, ISR 2007-26: WFC3 TV2 Testing: UVIS-2 Dark Frames and Rates

Robberto, M. 2007, ISR 2007-13: UVIS CCD EPER CTE Measurements in the April 2007 Ambient Calibration Campaign

Appendix A. Superbias Frame

Superbias files were generated from a sigma-clipped median of all TV2 good full-frame, four-amp readout, gain 1.5 biases, one superbias per instrument side (total of 78 images for MEB1 and 40 images for MEB2). Prior to stacking, the individual images were processed through the OPUS *calwf3* calibration routine to perform the overscan correction only. The result for MEB1 is shown in Fig. 5. Similar to the ambient data superbias image, the TV2 superbias overall is relatively flat in the A and B quadrants and shows some "ridges" or diffuse features (400-500 pixels wide, ~0.05-0.1 DN above the level of quadrant center) running parallel to the vertical outer edges. These bars were also discussed in Martel (2007; see their Fig. 2) in context of the dark frames.

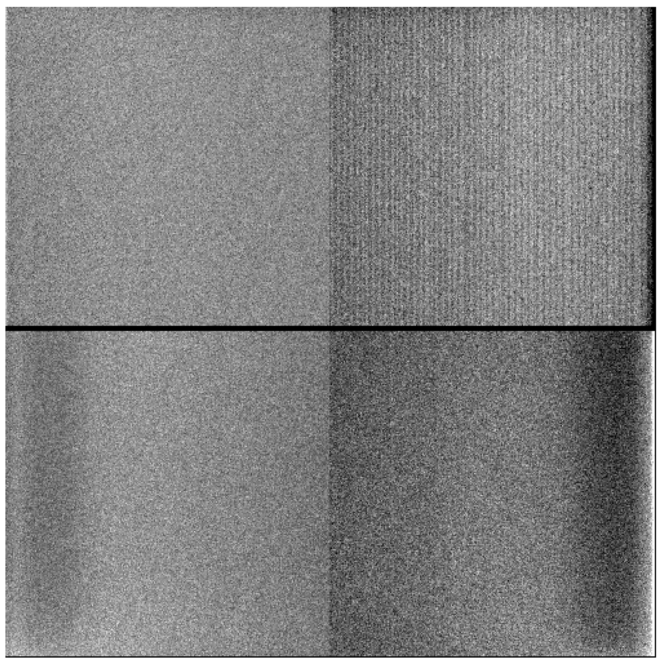

Figure 5 : Superbias frame for MEB1.

Images taken with the two instrument sides (MEB1, MEB2) yielded superbias images with similar overall features though the absolute levels were slightly different. Table 2 below lists the superbias image statistics (in electrons) of each quadrant (excluding outer 10 rows and columns as well as 3x sigma-clipped). Quadrants A and B have slightly lower levels on side 1 (MEB1) than on side 2 while quadrants C and D have slightly higher levels on side 1 than side 2.

Table 2 : Statistics of Superbias Frames (in e^-)

Quadrant	Side	Mean	Std Dev	Min	Max	Median
A	1	0.10	0.35	-0.97	1.17	0.04
A	2	0.15	0.65	-1.80	2.10	0.23
B	1	0.14	0.55	-1.50	1.78	0.14
B	2	0.17	0.71	-1.97	2.31	0.25
C	1	0.14	0.42	-1.12	1.39	0.24
C	2	0.13	0.53	-1.47	1.73	0.08
D	1	0.25	0.53	-1.35	1.84	0.34
D	2	0.23	0.74	-2.00	2.46	0.25

Finally, we note that as seen in the ambient data for UVIS-2 (Baggett 2007a), there appears to be a residual odd/even column effect in the superbias files that is not removed with the current *calwf3* overscan subtraction algorithm. Fig. 6 shows representative cuts through each quadrant: the average of rows 10-2041 across a sample of 50 columns. The effect is most prominent in quadrant B, where the level of the odd/even pattern is ~0.25 DN (~0.38 electrons) peak to peak; the other quadrants show hints of the pattern at 0.01-0.02 DN (0.01-0.03 electrons). Quadrant B has been known to show other anomalies which can be addressed via a change in the CCD gate voltages; the new voltages do not, however, remove the odd/even pattern.

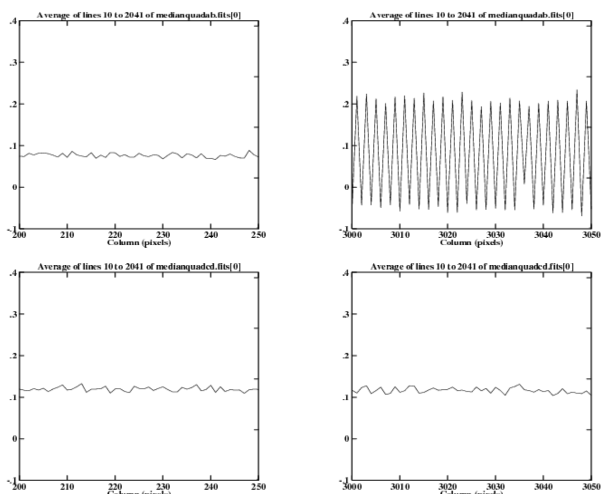

Figure 6 : Odd/even column effect in the superbias frames.

Since the odd/even behavior is present in the overscan region as well, it may be possible to remove it via the overscan correction, particularly useful if the pattern should switch parity over time (it did not during the relatively short duration of TV2). Currently, *calwf3* performs a line fit to the overscan regions; instead, separate fits to odd and even column overscans could be performed and removed from the science pixels. The efficacy of such an odd/even column-based overscan correction must still be investigated.